Side-Chain Dynamics of a Detergent-Solubilized Membrane Protein: Measurement of Tryptophan and Glutamine Hydrogen-Exchange Rates in M13 Coat Protein by ^{1}H NMR Spectroscopy†

Joe D. J. O'Neil‡ and Brian D. Sykes*

MRC Group in Protein Structure and Function, Department of Biochemistry, University of Alberta, Edmonton, Alberta T6G 2H7, Canada

Received December 16, 1988; Revised Manuscript Received April 25, 1989

ABSTRACT: M13 coat protein is a small (50 amino acids) lipid-soluble protein that becomes an integral membrane protein during the infection stage of the life cycle of the M13 phage and is therefore used as a model membrane protein. To study side-chain dynamics in the protein, we have measured individual hydrogen-exchange rates for a primary amide in the side chain of glutamine-15 and for the indole amine of tryptophan-26. The protein was solubilized with the use of perdeuteriated sodium dodecyl sulfate (SDS), and hydrogen-exchange rates were measured by using ^{1}H nuclear magnetic resonance spectroscopy. The glutamine-15 syn proton exchanged at a rate identical with that in glutamine model peptides except that the pH corresponding to minimum exchange was elevated by about 1.5 pH units. The tryptophan-26 indole amine proton exchange was biphasic, suggesting that two populations of tryptophan-26 exist. Approximately one-fourth of the tryptophan-26 resonance intensity exchanged at the same rate as a tryptophan model peptide, whereas three-fourths of the tryptophan-26 resonance intensity exchanged about 1000-fold more slowly. It is suggested that the two populations may reflect protein dimerization or aggregation in the SDS micelles. The pH values of minimum exchange for tryptophan-26 in both environments were also elevated by 1.3–1.9 pH units. This phenomenon is reproduced when small tryptophan- and glutamine-containing hydrophobic peptides are dissolved in the presence of SDS micelles. The electrostatic nature of this phenomenon is proven by showing that the minimum pH for exchange can be reduced by dissolving the hydrophobic peptides in the positively charged detergent micelle dodecyltrimethylammonium bromide. A small hydrophobic effect, which involves the depression of base catalysis to a significantly greater extent than acid catalysis, was observed for some of the peptides solubilized with the neutral detergent octyl glucoside.

In polypeptides the backbone amide is a very weak acid ($pK_a \simeq 18.5$) that will exchange its hydrogen with a protic solvent. In folded protein molecules it has been recognized for a long time that the rates of exchange of backbone amide protons are partly determined by the magnitude of the structural fluctuations within the molecule (Hvidt & Linderstrøm-Lang, 1954; Linderstrøm-Lang & Schellman, 1959). Most of the polar amino acids in proteins contain labile protons whose exchange might be used to measure the local dynamics of the side chains in addition to the chemical and physical properties of their microenvironments. In the absence of structure these side-chain protons exchange too rapidly to be easily measured because their pK_a values are low compared to the pK_a values of water (15.7) and H_3O^+ (−1.7) [see Eigen (1964)]. In addition, their exchange is potentially complicated by general catalysis by buffer ions and possibly by internal catalysis (Englander et al., 1972). Exceptions to these are the primary amides of Gln and Asn ($pK_a \simeq 15$; Allinger et al., 1976) and the secondary indole amine of tryptophan ($pK_a \simeq 17.5$; Waelder & Redfield, 1977), but even these side chains exchange faster than the polypeptide backbone amides. On the other hand, hydrogen-exchange studies of rhodopsin have suggested that the protein slows the exchange of as many as 40% of the proteins non-amide side chains (Englander et al., 1982).

Because the exchangeable indole proton of tryptophan usually resonates downfield from the rest of the protein's resonances, it is particularly convenient to measure individual amino acid exchange rates by using ^{1}H nuclear magnetic resonance (NMR)[1] spectroscopy. The exchange rates for the three slowest exchanging indoles in lysozyme were measured by Glickson et al. (1971). Importantly, these NMR experiments were among the first to show that some hydrogen-exchange rates are sensitive to the dynamic fluctuations involved in catalysis since the exchange rates are different in the presence and absence of substrate. Wedin et al. (1982) compared the individual indole proton exchange rates in lysozyme with the detailed microenvironment of each tryptophan in the static structure and concluded that a simple explanation of the exchange rates in terms of the burial and/or hydrogen bonding of the exchanging residues is inadequate. Tryptophan

†Supported by the Medical Research Council of Canada (MRC Group in Protein Structure and Function) and the Alberta Heritage Foundation for Medical Research (J.D.J.O. was the recipient of an AHFMR Postdoctoral Fellowship).

‡Present address: Department of Chemistry, University of Manitoba, Winnipeg, Manitoba R3T 2N2, Canada.

[1] Abbreviations: DE, direct exchange-out in D_2O; DMPC, dimyristoylphosphatidylcholine; DSS, disodium 2,2-dimethyl-2-silapentane-5-sulfonate; DOC, deoxycholate; DTAB, dodecyltrimethylammonium bromide; *f*, fractional amide intensity; HPLC, high-performance liquid chromatography; H_E, syn substituent of a primary amide; H_Z, anti substituent of a primary amide; k_{ex}, amide hydrogen-exchange rate; k_H, acid-catalyzed exchange rate constant; k_{min}, minimum exchange rate in exchange versus pH profile; k_{OH}, base-catalyzed exchange rate constant; K_W, equilibrium constant for the dissociation of water; NMR, nuclear magnetic resonance; OG, octyl glucoside (*n*-octyl β-D-glucopyranoside); pH_{min}, pH corresponding to k_{min} in exchange versus pH profile; pH^*_{min}, pH* corresponding to k_{min} in exchange versus pH* profile measured in D_2O; ppm, parts per million; pD, calculated deuterium ion activity in D_2O; pH*, pH meter reading in D_2O; SDS-d_{25}, perdeuteriated sodium dodecyl sulfate; ST, saturation transfer, T_1, spin–lattice relaxation time.

0006-2960/89/0428-6736$01.50/0

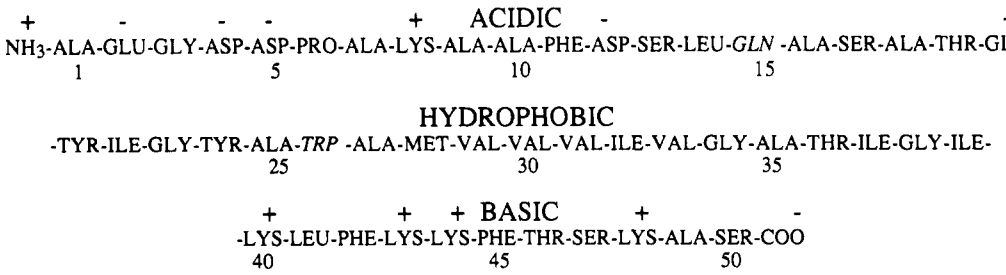

FIGURE 1: Amino acid sequence of M13 coat protein according to the findings of Asbeck et al. (1969) and Nakashima and Koningsberg (1974). Side-chain hydrogen-exchange rates are measured for Gln-15 and Trp-26, which reside in the acidic and hydrophobic segments, respectively.

side-chain exchange has also been measured in a number of model compounds (Waeleder & Redfield, 1977) and, recently, in other proteins by using NMR spectroscopy (Kawata et al., 1988) and Raman spectroscopy (Miura et al., 1988).

Tüchsen and Woodward (1987) measured side-chain amide exchange rates for Asn-43 and Asn-44 in bovine pancreatic trypsin inhibitor [see also Richarz et al. (1979)]. For these side chains amide exchange is slowed to such an extent (10^7- and 10^5-fold, respectively) that $N^\delta H_2$ rotation is faster than hydrogen exchange. Tüchsen and Woodward (1987) concluded that for exchange to occur dynamics involving more than simple hydrogen-bond breakage are necessary. Glutamine and asparagine side-chain amide exchange was also measured by Krishna et al. (1982) in *N*-acetylglutamine N_α-methylamide and in *N*-acetylasparagine N_α-methylamide in water. They confirmed that the acid-catalyzed reaction proceeds via N-protonation and that the proton anti to the amide carbonyl oxygen (H_E) exchanges faster than the syn proton (H_Z) just as in other primary amides (Perrin et al., 1981; Perrin & Arrhenius, 1982). Asparagine side-chain exchange has also been studied in a cyclic peptide (Narutis & Kopple, 1983) and in small peptides (Krishna et al., 1979).

During the reproductive cycle of the bacteriophage M13 (fd, f1) the major coat protein is inserted into the inner membrane of *Escherichia coli* (Webster & Cashman, 1978). The amino acid sequence of the protein (Asbeck et al., 1969; Nakashima & Konigsberg, 1974) includes a highly hydrophobic 19 amino acid core flanked by a 20-residue acidic N-terminal segment and an 11-residue basic C-terminus (Figure 1). A single glutamine is located in the amino-terminal region at position 15, and a single tryptophan is located at position 26 within the hydrophobic core. In the absence of dispersive agents, such as detergents and phospholipids, the coat protein is highly aggregated in water (Cavalieri et al., 1976) and there is evidence that the protein is a tightly associated dimer even in detergent micelles (Makino et al., 1975; Datema et al., 1987a,b, 1988). Individual backbone amide exchange rates of the protein, made soluble with SDS, have been measured by using a ^{13}C NMR equilibrium isotope-shift technique (Henry et al., 1987) as well as by ^{15}N NMR spectroscopy (Henry & Sykes, 1989). Exchange rates from about Ile-22 to Thr-46 (see Figure 1) are slower than in unstructured peptides by 10^3–10^6-fold, whereas in the rest of the molecule exchange is slowed by only 10–100-fold. Hydrogen-exchange studies using ^1H NMR spectroscopy confirmed that the hydrophobic core is very stable and that the hydrophilic termini are about 3 orders of magnitude less stable than the core (O'Neil & Sykes, 1988).

If protein dynamic information is to be deduced from the rates of hydrogen exchange in proteins, then the intrinsic chemical and physical contributions to exchange must be taken fully into account. Because M13 coat protein is solubilized with detergent, we examined the effects of detergent on the amide-exchange kinetics of a micelle-solubilized, amphipathic, "structureless" tripeptide, NH_3^+-Leu-Val-Ile-amide (O'Neil & Sykes, 1989). Those experiments showed that the main effect of dodecyl sulfate was to shift the minimum pH for exchange to higher pH by about 1.5 units. No large changes in k_{min}, the exchange rate at the pH_{min}, were measured. The changes in pH_{min} are due to an electrostatic effect of the sulfate residue of SDS which decreases the pH in the vicinity of the exchanging amides by condensing protons onto the surface of the detergent micelle. The opposite effect, shifting the pH_{min} to lower pH, could not be demonstrated because the positively charged peptide did not associate with the positively charged detergent DTAB. In this paper we have demonstrated just such a lowering of the pH_{min} for exchange of a negatively charged peptide, *N*-acetyl-Trp-Phe-COO^-, in DTAB.

The internal dynamics of membrane protein side chains have been the subject of considerable controversy (Lewis et al., 1985; Keniry et al., 1984). As a measure of the side-chain dynamics of SDS-solubilized M13 coat protein, we have determined hydrogen-exchange rates for an amino acid in the "acidic" amino terminus and for one in the membrane-spanning hydrophobic core. Gln-15 amide exchange is unhindered, whereas Trp-26 indole NH exchange is slower by a factor of 200–1000 and may be sensitive to protein self-association.

Experimental Procedures

Materials

DSS and perdeuteriated sodium dodecyl sulfate were purchased from MSD Isotopes (Pointe Claire, Dorval, PQ, Canada), and perdeuteriated acetic acid was from Stohler-Isotope Chemicals (Rutherford, NJ). D_2O was purchased from Bio-Rad Laboratories (Richmond, CA). Doxylstearic acid, labeled at carbon 12, was purchased from Molecular Probes (Junction City, OR). The DTAB, OG, and unblocked Trp-Phe were from Sigma Chemical Co. (St. Louis, MO). The peptide Trp-Phe was acetylated by using acetic anhydride in pyridine according to the method of Means and Feeney (1971). *N*-Acetyl-L-Trp-amide was from Aldrich Chemical Co. (Milwaukee, WI). The peptide *N*-acetyl-Leu-Gln-Ile-amide was purchased from the Alberta Peptide Institute. Its purity was checked by ^1H NMR spectroscopy and HPLC.

Methods

Exchange-Out of Trp-26 Indole NH. Bacteriophage M13 growth and M13 coat protein preparation were as described by O'Neil and Sykes (1988). Briefly, coat protein in SDS-d_{25} and disodium phosphate, buffered at pH 7, was freeze-dried. Exchange, at various pH values, was initiated by dissolving the freeze-dried protein in D_2O and either acetate or borate buffer. Hydrogen exchange was followed by acquiring ^1H NMR spectra of the freshly dissolved protein, in 5-mm NMR tubes, with a Varian XL-400 NMR spectrometer. The pulse width was 12 μs (60°), and the acquisition time was 1 s. The number of acquisitions was 200 or 500. Protein concentration was 1.5 mM.

Saturation-Transfer Measurements of Hydrogen Exchange. Most of the hydrogen-exchange rates reported in this paper were too rapid to have been measured by direct exchange-out methods. To measure rapidly exchanging amides in M13 coat protein as well as in small peptides, we have used an NMR technique in which proton spectra are obtained in water and the solvent peak is eliminated with preirradiation (Forsen & Hoffman, 1963, 1964; Perrin & Johnson, 1979; Gadian, 1982). For those protons whose longitudinal relaxation rates ($1/T_1$) are of the order of or less than their hydrogen-exchange rates (k_{ex}), saturation of the solvent resonance will be carried over to the protein and diminish the intensity of the exchangeable proton resonance accordingly

$$f = 1/(1 + k_{ex}T_1) \quad (1)$$

where f is the ratio of the NH intensity in the presence of solvent irradiation to the intensity in the absence of irradiation. The standard inversion recovery experiment was used to measure the T_1 values at the pH_{min} where $k_{ex} \ll 1/T_1$. Sometimes, however, k_{ex} was of the order of $1/T_1$, even at the pH_{min} where exchange was slowest. In this situation the measured relaxation rate ($1/T_1^{obs}$) is greater than the intrinsic rate ($1/T_1$), accordingly

$$1/T_1^{obs} = 1/T_1 + k_{ex} \quad (2)$$

Thus, f was determined by measuring the proton intensity in the presence and absence of solvent irradiation. Then $1/T_1$ was calculated from the measured relaxation rate ($1/T_1^{obs}$) and measured f value by using eq 1 and 2. In addition, since hydrogen exchange is acid- and base-catalyzed, measurement of the pH dependence of the fractional amide intensity gives acid- and base-catalyzed (k_H and k_{OH}, respectively) rate constants by use of eq 3, the pH_{min} by use of eq 4, and the rate at the minimum (k_{min}) by use of eq 5. The pH dependence

$$k_{ex} = k_{OH}[OH^-] + k_H[H_3O^+] \quad \text{or}$$
$$k_{ex} = k_{OH} \times 10^{pH-pK_W} + k_H \times 10^{-pH} \quad (3)$$

$$pH_{min} = \tfrac{1}{2}\, pK_W - \tfrac{1}{2} \log k_{OH}/k_H \quad (4)$$

$$k_{min} = 2k_H \times 10^{-pH_{min}} \quad (5)$$

of the M13 coat protein Trp-26 NH intensity data did not fit well to a single transition (eq 1), and these data were fitted to two transitions by using

$$f = \frac{f_1}{1 + k_{ex1}T_1} + \frac{1 - f_1}{1 + k_{ex2}T_1} \quad (6)$$

where f_1 and $1 - f_1$ are the changes in relative amide intensity due to each transition.

In the saturation-transfer experiments on the peptides an amount of peptide that would give a 1–2 mM solution was added to a solution of 15% D_2O/85% H_2O and 50 mM detergent. However, not all of the peptides were soluble at these concentrations, and the solutions were centrifuged to remove the insoluble material. Solutions also contained approximately 10 mM phosphate, 10 mM acetic acid-d_4, and, at higher pH values, 10 mM borate buffers. ^1H NMR spectra of these solutions in 5-mm NMR tubes were acquired with a Varian VXR-500 NMR spectrometer at 25 or 30 °C with preirradiation of the water resonance for 1.7 s. The (1,1) pulse sequence was used to acquire spectra without solvent irradiation (Plateau & Gueron, 1982). The pulse width was 14 μs (90°), and usually 100 scans were acquired for 1 s each. The standard inversion-recovery experiment was used to measure the T_1 values.

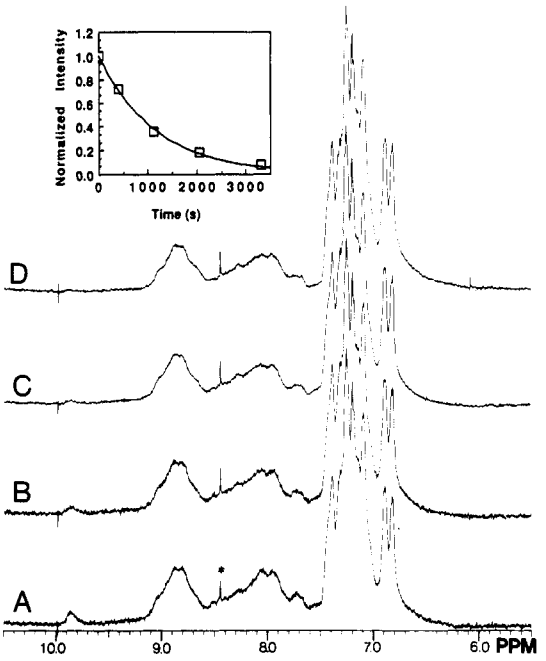

FIGURE 2: Low-field region of 400-MHz ^1H NMR spectra of M13 coat protein showing the time course of Trp-26 indole NH (9.86 ppm) exchange at (A) 5, (B) 17, (C) 30, and (D) 51 min after dissolution in D_2O and SDS-d_{25} at pH* 7.14 and 24 °C. The number of scans was 200 for (A) and (B) and 500 for (C) and (D). Inset shows fit of normalized intensity of indole NH resonance as a function of time ($k = 8.6 \times 10^{-4}$ s^{-1}). The protein concentration was 1.5 mM, and phosphate was 22 mM. A line broadening of 0.5 Hz was used in processing the spectra. The asterisk indicates a formate resonance.

The deuterium ion activity (pD) was not corrected for the glass electrode reading error (Glasoe & Long, 1960), and direct meter readings (pH*) are reported [for a discussion see Englander et al. (1979) and Bundi and Wüthrich (1979)]. Chemical shifts were measured relative to the methyl resonances of DSS.

Results

Exchange-Out of the Indole NH of Trp-26. Figure 2A shows the aromatic and amide regions of a ^1H NMR spectrum of M13 coat protein at 400 MHz acquired 5 min after dissolution of the protein in D_2O and SDS-d_{25} at pH* 6.74 and 24 °C [see O'Neil and Sykes (1988)]. The side-chain indole NH of Trp-26 appears in the spectrum at 9.86 ppm (Cross & Opella, 1980), completely resolved from the envelope of backbone amides that are all upfield in the spectrum (9.1–7.5 ppm). The resonance position of the indole NH is about 0.4 ppm upfield of the "random coil" position as measured in small peptides (Bundi & Wüthrich, 1979). The exchange experiment at pH* 6.74 was quantified by fitting the peak heights of the indole NH resonances at various times after dissolution (Figure 2A–D) to an exponential decay with a nonlinear least-squares fitting routine; the rate constant is given in Table I. Exchange was also measured at other pH* values but exchange at pH* 6.74 was the slowest measured, and this is near the practical limit of the direct exchange-out technique; exchange that has a $t_{1/2}$ of less than 5 min ($k_{ex} > 2 \times 10^{-3}$ s^{-1}) cannot be measured. Indeed below pH* 6.42 and above pH* 7.84 no Trp-26 indole NH was ever observed in spectra of the protein in D_2O. Exchange at pH* 6.42, 7.50, and 7.84 was near the exchange limit, and estimates of the exchange rate at these pH* values are also given in Table I. These experiments give an estimate of the pH^*_{min} ($\simeq$6.7) and the exchange rate, k_{min}, at the pH^*_{min} (8.6×10^{-4} s^{-1}). The pH^*_{min} is higher by about 1.6 pH units and the k_{min} about 200-fold

Table I: Summary of Hydrogen-Exchange Measurements on the Side Chains of Gln-15 and Trp-26 of M13 Coat Protein in SDS-d_{25}[a]

		T_1 (s)	f	k_{OH} (M^{-1} s^{-1})	k_H (M^{-1} s^{-1})	k_{min} (s^{-1})	pH_{min}	k_{ex} (s^{-1})	pH*
Gln-15(H_Z)	ST	0.56		$(1.1 \pm 0.1) \times 10^{-6}$	$(5.7 \pm 0.9) \times 10^{4}$	4.9×10^{-2}	6.37		
Trp-26 indole a	ST	1.01	0.78 ± 0.02	1827 ± 256	378 ± 54	1.6×10^{-4}	6.66		
Trp-26 indole b	ST	1.01	0.27 ± 0.04	$(1.2 \pm 0.8) \times 10^{6}$	$(8.9 \pm 5.6) \times 10^{5}$	0.66	6.43		
Trp-26 indole	DE							$\simeq 2 \times 10^{-3}$	6.42
Trp-26 indole	DE							8.6×10^{-4}	6.74
Trp-26 indole	DE							$<3 \times 10^{-3}$	7.50
Trp-26 indole	DE							$<3 \times 10^{-3}$	7.84

[a] The pH dependence of NH intensity due to saturation transfer (ST) shown in Figure 4 was fit to eq 1 (Gln-15) or eq 6 (Trp-26) in the text by using the T_1 values given in the table. k_{OH} and k_H are the first-order catalytic rate constants determined from the fits. The errors are the calculated standard deviations of the fits. The pH_{min} and k_{min} were calculated by using eq 4 and 5, respectively. Protein was about 2.5 mM in SDS-d_{25} and 85% H_2O/15% D_2O at 25 °C. For the direct exchange-out into D_2O experiments (DE) the estimated exchange rate (k_{ex}) at each pH* is given.

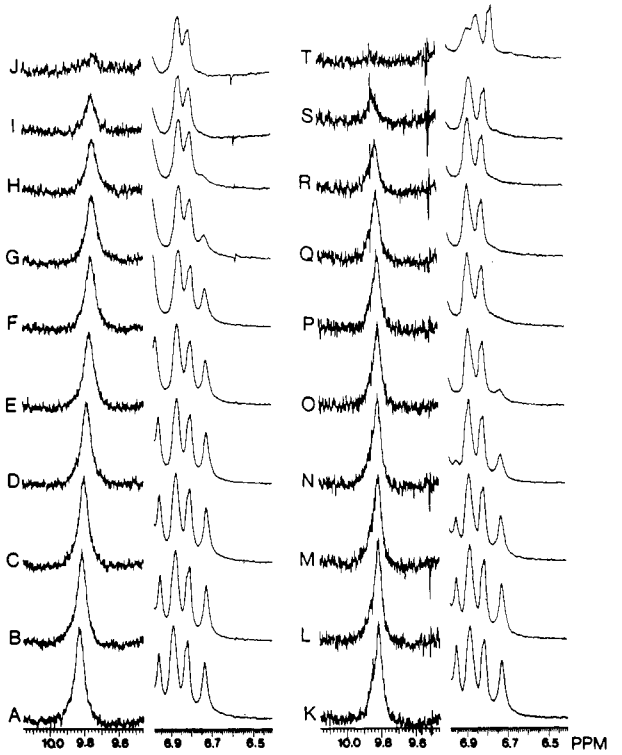

FIGURE 3: Low-field regions of 500-MHz ^1H NMR spectra of M13 coat protein showing the pH dependence of NH intensities at pH (A) 6.80, (B) 6.46, (C) 5.98, (D) 5.56, (E) 5.10, (F) 4.52, (G) 3.65, (H) 2.99, (I) 2.53, (J) 1.95, (K) 6.95, (L) 7.40, (M) 7.81, (N) 8.33, (O) 8.95, (P) 9.37, (Q) 9.95, (R) 10.44, (S) 10.90, and (T) 11.50. The Trp-26 indole NH proton resonates at 9.82 ppm, and the Gln-15 side-chain H_Z resonates at 6.73 ppm. Spectra were acquired for 1.0 s with preirradiation of the solvent resonance for 1.5 s in 85% H_2O/15% D_2O. The number of scans was 200, and the pulse width was 17 μs (90°). The protein concentration was 2.7 mM in SDS-d_{25}, 100 mM phosphate, and 11 mM acetic acid-d_4 in (A–J) and 12 mM borate in (K–T). A line broadening of 0.5 Hz was used in processing the spectra.

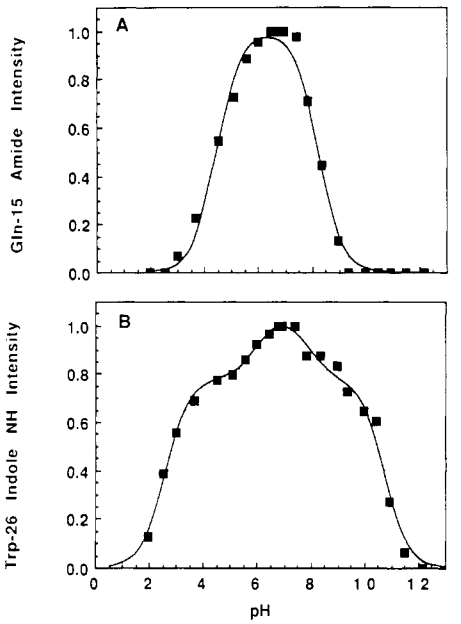

FIGURE 4: pH dependence of NH intensity due to saturation transfer for (A) the side-chain H_Z of Gln-15 and (B) the indole NH of Trp-26 in M13 coat protein solubilized with SDS-d_{25}. The peak heights in Figure 3 are plotted vs pH; the lines through the points are nonlinear least-squares fits of the data as described in the text by using eq 1 for (A) and eq 6 for (B). The T_1 values are given in Table I; k_{ex} was calculated by using eq 3. In Figure 6B the major transition (f_1) accounted for 74% of the loss in NH intensity, and the minor transition ($1 - f_1$) accounted for 26% of the loss.

slower than similar measurements for Trp in small peptides in an aqueous environment [see Nakanishi et al. (1978) and Table III). No primary amide protons from Gln-15 were ever observed in any of the spectra acquired in D_2O.

Trp-26 and Gln-15 Exchange Measured by Saturation Transfer. Spectra A and K in Figure 3 are the downfield regions of ^1H NMR spectra at 500 MHz of M13 coat protein in 15% D_2O/85% H_2O at pH 6.80 and 6.92, respectively. The indole NH of Trp-26 resonates at 9.85 ppm in these spectra; the sharp singlet at 6.75 ppm, which partially overlaps a tyrosine aromatic resonance ($C_{3,5}H$), is assigned to Gln-15. The singlet at 6.75 ppm is entirely absent from spectra in D_2O and resonates close to the random coil position (6.88 ppm) of the primary amide (H_Z) of the Gln side chain (Bundi & Wüthrich, 1979). Only one amino acid in M13 coat protein (Figure 1) contains a primary amide, and we therefore assume that the resonance at 6.75 ppm arises from Gln-15; since the H_Z (syn) substituent almost always resonates at a higher field than the H_E (anti) substituent (Perrin et al., 1980), we assume that the E substituent resonates in the aromatic region of the spectrum (6.8–7.5 ppm) and assign the resonance at 6.75 ppm to the H_Z substituent of the Gln-15 side chain.

Small amounts of HCl and NaOH in 15% D_2O/85% H_2O were added to the solutions corresponding to spectra A and K in Figure 3, respectively. Figure 3 shows the reduction in NH intensity for the side chains of Gln-15 and Trp-26 due to acid- (A–J) and base-catalyzed (K–T) exchange and concomitant saturation transfer. The pH dependence of the peak heights are shown in Figure 4, parts A and B, for Gln-15 and Trp-26, respectively. The Gln-15 data were fit with a nonlinear least-squares routine to eq 1 by using eq 3 for k_{ex} and the T_1 given in Table I. The values for k_{OH} and k_H, determined from the fit, are listed in Table I; these values were used to calculate pH_{min} and k_{min} by using eq 4 and 5, respectively (Table I). The exchange rate (k_{min}) at the pH_{min} for Gln-15 is similar to the value calculated from the results of Krishna et al. (1982) for *N*-acetyl-Gln N_α-methylamide (see also Table II). This suggests that exchange of the side chain of Gln-15 in the

Table II: Summary of the Hydrogen-Exchange Kinetics for the Primary Amides in *N*-Acetyl-Leu-Gln-Ile-amide[a]

			T_1 (s)	k_{OH} (M^{-1} s^{-1})	k_H (M^{-1} s^{-1})	k_{min} (s^{-1})	pH_{min}	ΔpH_{min}
I	Q-$NH_2(H_Z)$	H_2O	0.72	$(4.1 \pm 0.3) \times 10^7$	$(3.6 \pm 0.2) \times 10^3$	7.7×10^{-2}	4.97	
I	Q-$NH_2(H_Z)$	SDS	0.58	$(5.5 \pm 0.6) \times 10^6$	$(5.9 \pm 0.7) \times 10^4$	11.5×10^{-2}	6.01	1.05
I	Q-$NH_2(H_Z)$	DTAB	0.75	$(2.1 \pm 0.9) \times 10^7$	$(3.8 \pm 0.2) \times 10^3$	5.6×10^{-2}	5.13	0.16
I	Q-$NH_2(H_Z)$	OG	0.75	$(1.8 \pm 0.3) \times 10^7$	$(4.5 \pm 0.8) \times 10^3$	5.8×10^{-2}	5.19	0.22
I	$CONH_2(H_Z)$	H_2O	0.48	$(9.3 \pm 0.5) \times 10^7$	221 ± 11	2.9×10^{-2}	4.19	
I	$CONH_2(H_Z)$	SDS	0.47	$(2.0 \pm 1.0) \times 10^7$	$(5.8 \pm 0.4) \times 10^3$	6.8×10^{-2}	5.23	1.04
I	$CONH_2(H_Z)$	DTAB	0.51	$(6.9 \pm 0.5) \times 10^7$	367 ± 27	3.2×10^{-2}	4.36	0.17
I	$CONH_2(H_Z)$	OG	0.47	$(6 \pm 1) \times 10^7$	519 ± 134	3.4×10^{-2}	4.48	0.29

[a] The pH dependence of NH intensity due to saturation transfer shown in Figure 5 was fit to eq 1 in the text by using the T_1 values given in the table. ΔpH_{min} = pH_{min}(detergent) − pH_{min}(water). Q-$NH_2(H_Z)$ indicates the syn proton of the Gln side chain in *N*-acetyl-Leu-Gln-Ile-NH_2 (I). $CONH_2(H_Z)$ indicates the syn proton at the carboxy terminus of the same peptide (I). H_2O designates experiments carried out in 85% H_2O/15% D_2O. SDS designates experiments done in 85% H_2O/15% D_2O and 50 mM SDS-d_{25}. DTAB designates experiments done similarly in 50 mM dodecyltrimethylammonium bromide. OG designates experiments done similarly in 50 mM octyl glucoside. All experiments were done at 25 °C. All other symbols are as in the legend to Table I.

protein is unhindered by either the structure of the protein or the detergent. On the other hand, the pH_{min} for Gln-15 is elevated by about 1.4 pH units compared to the value calculated from the results of Krishna et al. (1982) (see also Table II).

The pH dependence of the single indole NH intensity from Trp-26 (Figure 4B) did not fit well to a single acid- and base-catalyzed transition, and these data were fit to two such transitions by using eq 6 and the T_1 value given in Table I. The major transition, accounting for about 74% of the loss in NH intensity, yielded a k_{min} about 5-fold slower than the slowest exchange measured by exchange-out into D_2O (see Table I). This is about 1000-fold slower than the k_{min} measured for Trp model compounds by Nakanishi et al. (1978) and by Waeleder and Redfield (1977) (see also Table III). The pH_{min} for this transition is similar to the estimated pH^*_{min} measured by the exchange-out technique (Table I) and is 1.6–1.9 pH units higher than the minima measured for Trp model compounds in water [see Nakanishi et al. (1978), Waeleder and Redfield (1977), and Table III].

The minor pH transition accounts for about 26% of the loss in the indole NH intensity of Trp-26 (Figure 4B; Table I). The saturation-transfer-determined k_{min} (0.66 s^{-1}) is much too fast to be measured directly and is not observed in the direct exchange-out into D_2O experiment (Table I). The rate of exchange at the pH_{min} for this transition is 2–3-fold greater than the measured k_{min} for free Trp (see Table III; Nakanishi et al., 1978; Waeleder & Redfield, 1977). As the scatter in the data in Figure 4B and the errors in Table I show, there is some uncertainty in the kinetic parameters determined for the minor transition, and it is concluded that this transition reflects unhindered Trp exchange. It is not known if the two observed transitions have different relaxation rates. For example, if the T_1 for the minor transition was greater than 1.0 s, then k_{min} would be overestimated in Table I. The pH_{min} (6.43) for the minor transition is similar to that of the major transition (6.66) and is 1.3–1.7 pH units higher than pH_{min} measured for freely exchanging Trp (see Table III; Nakanishi et al., 1978; Waeleder & Redfield, 1977).

Hydrogen Exchange in Small Peptides. Many of the hydrogen-exchange kinetic parameters measured for Gln-15 and Trp-26 are significantly different from those of model amino acids exchanging in water. These differences arise from the influence of protein structure as well as from environmental factors such as the detergent molecules, which can significantly influence exchange (O'Neil & Sykes, 1989). To measure the effects of detergent on exchange of the side chains, exchange was measured for small "unstructured" peptides in a variety of aqueous and detergent environments. Figure 5A shows the pH dependences of the H_Z amide intensities in *N*-acetyl-

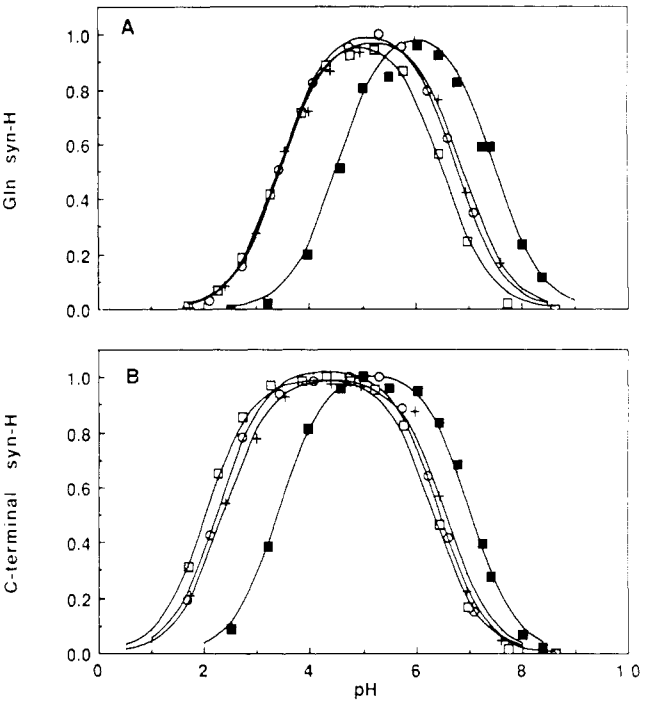

FIGURE 5: pH dependence of primary amide intensity due to saturation transfer in *N*-acetyl-Leu-Gln-Ile-NH_2 for (A) the glutamine side-chain H_Z and (B) the carboxyl-terminal H_Z. The lines through the points are nonlinear least-squares fits of the data using eq 1 in the text and the T_1 values given in Table II. The peptide was in (□) water, (■) SDS-d_{25}, (○) DTAB, or (+) OG. All experiments were done at 25 °C.

Leu-Gln-Ile-NH_2 in water, SDS, DTAB, and OG. The kinetic parameters from the nonlinear least-squares fits of the data as well as the calculated k_{min} and pH_{min} values are given in Table II. The measured T_1 values show little variation with environment, except for the Gln H_Z proton T_1 that is smaller in SDS. The differences in k_{min} due to detergent are relatively small, and when they are accompanied by changes in pH_{min}, they show that k_{OH} has changed more or less than k_H has changed. The largest change (1.05) is seen in the pH_{min} when the peptide is dissolved in SDS; k_{min} in SDS is elevated somewhat, and this is because the enhancement in k_H due to SDS is measurably greater than the suppression of k_{OH}. In addition, the resonant frequencies of the amide protons shift when the peptide is dissolved in SDS; for example, whereas all of the primary amide protons are well resolved in the water spectrum, the carboxyl-terminal and side-chain H_E resonances overlap in SDS at 7.49 ppm (not shown). The same is true of the spectrum of the peptide dissolved in OG; the two H_E's resonate at 7.50 ppm. Although OG appears to elevate the

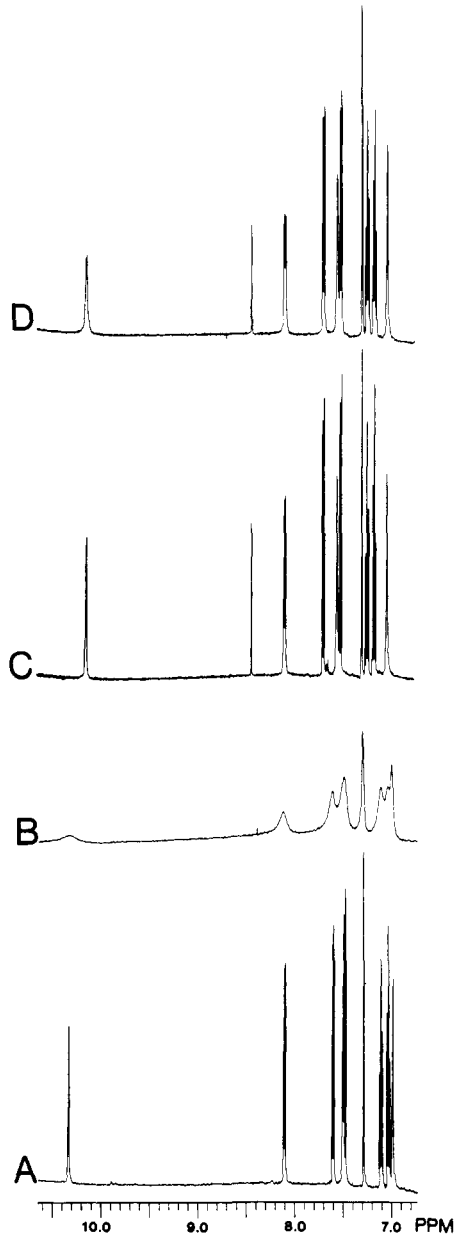

FIGURE 6: Low-field region of 500-MHz ^1H NMR spectra of *N*-acetyl-Trp-NH_2 in (A, B) DTAB and in (C, D) OG in the (A, C) absence and (B, D) presence of 12-doxylstearic acid. The amino acid in DTAB at pH 4.71 (A) was exposed to spin-labeled fatty acid (B) at a mole ratio of DTAB:12-DS = 200:1, and then the sample was centrifuged to remove insoluble material. The amino acid in OG at pH 5.01 (C) was exposed to spin label (D) at a mole ratio of OG:12-DS = 300:1, but judging from the cloudiness of the sample, most of the spin-labeled fatty acid was removed by subsequently centrifuging the sample. Each spectrum is the average of 100 scans acquired in 15% D_2O/85% H_2O with a pulse width of 13 μs (90°). No line broadening or resolution enhancement was used in the processing of the spectra.

pH_{min} to a small extent and to slightly reduce k_{min} of the Gln side-chain amide by depressing k_{OH} slightly more than k_H is enhanced (Table II), the change in k_H is not significant when the errors in the measurements are taken into account. The pH_{min} of the carboxyl-terminal amide is also elevated in OG, but in this case it appears that k_{min} is slightly elevated and k_{OH} is depressed to a slightly smaller extent than k_H is enhanced.

The kinetic parameters of the peptide *N*-acetyl-Leu-Gln-Ile-NH_2 in DTAB are similar to those measured in water (Figure 5; Table II), and the ^1H NMR chemical shifts of the primary amide protons in DTAB are also very similar to those in water (not shown). This suggests that the interaction between the neutral peptide and positively charged detergent is weak. Since the peptide was in short supply, no experiments with spin-labeled fatty acid were done to verify the location of the peptide (see below).

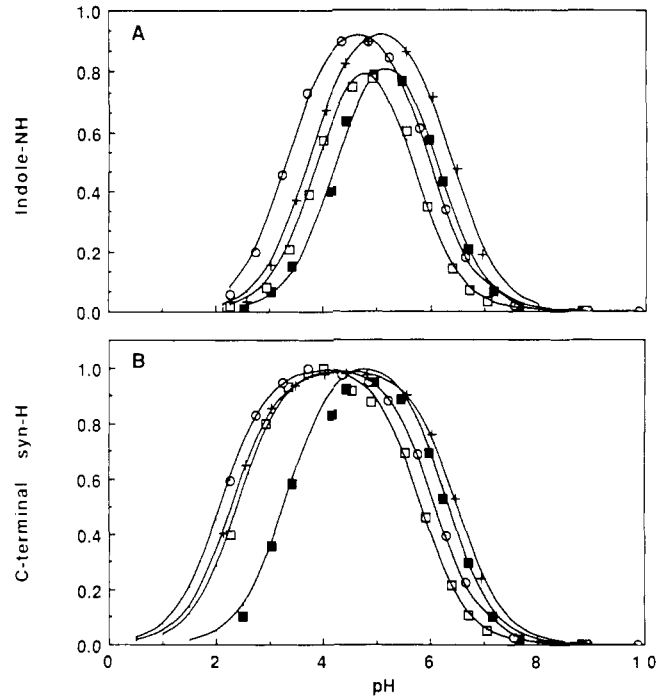

FIGURE 7: pH dependence of NH intensity due to saturation transfer in *N*-acetyl-Trp-amide for (A) the side-chain indole NH and (B) the carboxyl-terminal H_Z. The lines through the points are nonlinear least-squares fits of the data using eq 1 in the text and the T_1 values in Table III. The peptide was in (□) water, (■) SDS-d_{25}, (○) DTAB, or (+) OG. All titrations were done at 30 °C except for the experiment in OG, which was done at 25 °C.

The exchange kinetics of the amino acid *N*-acetyl-Trp-NH_2 were also studied in all four environments. The relaxation rates ($1/T_1$) for the indole NH and primary amides increased significantly when the amino acid was solubilized in each of the detergents (Table III); the resonant frequencies of the exchangeable protons also shifted when the peptide was solubilized with SDS and DTAB (not shown). Further evidence that the blocked amino acid was interacting with detergent was obtained by adding 12-doxylstearate to a solution containing formate, detergent, and the amino acid. In general, the spin label broadened the resonances of the amino acid and the detergent (not shown) but did not alter the formate resonance which is excluded from detergent micelle (O'Neil & Sykes, 1989). The experiments with the amino acid in DTAB and OG are shown in Figure 6. Similar to the experiment in SDS (not shown), the spin label broadened the resonances of both the amino acid and the DTAB, suggesting a close interaction between the DTAB-solubilized spin label and the amino acid (Figure 6A,B). However, the spin label was not very soluble in the neutral detergent, OG, and the amino acid and detergent resonances were only slightly broadened (e.g., indole NH, $\Delta\nu_{1/2}$ = 5.78 Hz, Figure 6C; $\Delta\nu_{1/2}$ = 10.32 Hz, Figure 6D). In this experiment the formate resonance was also slightly broadened by the spin label ($\Delta\nu_{1/2}$ = 1.02 Hz, Figure 6C; $\Delta\nu_{1/2}$ = 1.43 Hz, Figure 6D), so this experiment was inconclusive about the location of the amino acid with respect to the detergent.

The largest effect on the kinetics of exchange of both the indole NH and the terminal amide of *N*-acetyl-Trp-NH_2 was caused by SDS (Figure 7; Table III). In each case the pH_{min} and k_{min} were elevated, the enhancement in k_H being slightly

Table III: Summary of the Hydrogen-Exchange Kinetics for the Indole NH's and Primary Amides in *N*-Acetyl-Trp-NH_2 (II) and *N*-Acetyl-Trp-Phe (III)[a]

			T_1 (s)	k_{OH} (M^{-1} s^{-1})	k_H (M^{-1} s^{-1})	k_{min} (s^{-1})	pH_{min}	ΔpH_{min}
II	$CONH_2(H_Z)$	H_2O	0.82	$(1.8 \pm 0.1) \times 10^8$	317 ± 28	0.06	4.04	
II	$CONH_2(H_Z)$	SDS	0.53	$(9.15 \pm 0.06) \times 10^7$	$(3.8 \pm 0.3) \times 10^3$	0.14	4.73	0.69
II	$CONH_2(H_Z)$	DTAB	0.50	$(1.58 \pm 0.04) \times 10^8$	243 ± 9	0.05	4.01	−0.03
II	$CONH_2(H_Z)$	OG	0.59	$(5.1 \pm 0.1) \times 10^7$	332 ± 9	0.03	4.40	0.36
II	indole	H_2O	1.54	$(1.3 \pm 0.1) \times 10^8$	$(5.2 \pm 0.4) \times 10^3$	0.20	4.72	
II	indole	SDS	1.02	$(7.4 \pm 0.7) \times 10^7$	$(1.7 \pm 0.2) \times 10^4$	0.27	5.10	0.38
II	indole	DTAB	0.97	$(1.1 \pm 0.5) \times 10^8$	$(2.1 \pm 0.1) \times 10^3$	0.11	4.57	−0.15
II	indole	OG	1.10	$(5.1 \pm 0.3) \times 10^7$	$(7.2 \pm 0.4) \times 10^3$	0.15	4.99	0.27
III	indole	H_2O	0.97	$(9 \pm 2) \times 10^7$	$(1.2 \pm 0.4) \times 10^4$	0.21	5.06	
III	indole	SDS	0.87	$(2.6 \pm 0.5) \times 10^7$	$(7 \pm 1) \times 10^4$	0.3	5.70	0.64
III	indole	DTAB	0.77	$(4.3 \pm 0.2) \times 10^7$	78 ± 4	0.01	4.12	−0.94

[a] The pH dependence of NH intensity due to saturation transfer shown in Figures 7 and 8 was fit to eq 1 in the text by using the T_1 values given in the table. II designates *N*-acetyl-Trp-NH_2, and III designates *N*-acetyl-Trp-Phe. The experiments on II were done at 30 °C except for those in OG, which were done at 25 °C; the kinetic parameters for II in OG were multiplied by 1.5 for ease of comparison to the results at 30 °C. The experiments on III in H_2O and SDS were done at 25 °C, and those in DTAB were done at 30 °C; the kinetic parameters for III in DTAB were therefore divided by 1.5. All other symbols are defined in the legends to Tables I and II.

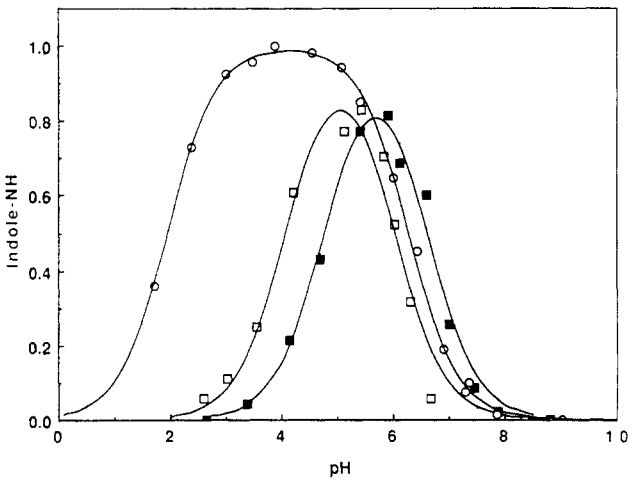

FIGURE 8: pH dependence of indole NH intensity due to saturation transfer in *N*-acetyl-Trp-Phe. The lines through the points are nonlinear least-squares fits of the data using eq 1 in the text and the T_1 values given in Table III. The peptide was in (□) water or (■) SDS-d_{25} at 25 °C or in (○) DTAB at 30 °C. Titrations of the peptide in DTAB at 25 °C were similar to that shown in this figure at 30 °C.

greater than the suppression of k_{OH}. OG also elevated the pH_{min} but reduced the k_{min} of both protons, and in both cases the largest effect is on k_{OH} (Table III). DTAB had a larger influence on the indole NH than on the terminal amide, but the decreases in pH_{min} and k_{min} are very small (Table III).

The positively charged detergent DTAB had the greatest effect on the exchange kinetics of the negatively charged *N*-acetyl-Trp-Phe (Figure 8; Table III). As Table III also shows, DTAB increased the relaxation rate of the indole NH. In addition, the indole NH resonance appeared as a partially overlapping doublet in the ^1H NMR spectrum (not shown), suggesting that in DTAB the indole exists in two conformations and that the peptide may form a dimer. In fact, all of the exchangeable proton resonances in *N*-acetyl-Trp-Phe were doublets in both SDS and DTAB (not shown). Both the pH_{min} and k_{min} were reduced by the positively charged detergent mainly due to a 15-fold suppression of k_H; k_{OH} was also slightly suppressed in DTAB (Table III). Similar to all the other peptides in SDS, the pH_{min} and k_{min} of the indole NH in *N*-acetyl-Trp-Phe are elevated (Figure 8; Table III).

Discussion

Exchange from the Coat Protein. An earlier study of backbone amide hydrogen-exchange rates in M13 coat protein (O'Neil & Sykes, 1988) concluded that the hydrophobic segment of the protein (Figure 1) contains the most slowly exchanging amides. At that time individual amide resonances were not resolved in the ^1H NMR spectra, so that assignment of the most slowly exchanging amides to the core of the protein was done by proteolyzing the protein with proteinase K and measuring exchange from the intact hydrophobic core. The slowest exchanging amides exchanged with an elevated pH^*_{min} and with an average rate that was about 10^5-fold slower than the exchange of freely exchanging model compounds. Backbone amides in the acidic and basic termini of the protein (Figure 1) were slower by only 10–100-fold compared with the rates of exchange of freely exchanging amides; the rapidly exchanging amides also exchanged with an elevated pH^*_{min}.

Glutamine-15 resides in the acidic amino terminus of the protein (Figure 1), where the backbone amides have been observed to exchange relatively rapidly (O'Neil & Sykes, 1988; Henry et al., 1987). The saturation-transfer measurements (Figures 3 and 4) of the side-chain H_Z in Gln-15 show that it exchanges at about the same rate as that of freely exchanging glutamine in model compounds. The conclusion is that the Gln-15 side chain is not hydrogen-bonded to another part of the protein nor is the detergent micelle or the structure of the protein able to restrict access of the side chain to ionized water molecules. However, the pH_{min} for exchange of the side-chain amide is elevated by about 1.4 pH units (Table I) compared to the pH_{min} for water-solubilized glutamine-containing model compounds (Table II). As Table II and Figure 5 show, an SDS micelle can interact with a hydrophobic peptide and elevate the pH_{min} of a glutamine side chain by about 1 pH unit. The micelle does this by concentrating protons near its negatively charged surface, thereby enhancing acid-catalyzed exchange and inhibiting base-catalyzed exchange. The magnitude of the pH_{min} elevation in the protein (1.4 pH units) suggests that the Gln-15 side chain spends more time closer to the surface of the micelle than does the glutamine in *N*-acetyl-Leu-Gln-Ile-NH_2, whose pH_{min} is elevated by 1 pH unit (Table II). We know Gln-15 is not inside the micelle since the amino-terminal region can be digested with proteinase K. It is also possible that the Gln-15 amide resides in a region of high negative charge density owing to additional contributions from the five acidic amino acids in the amino terminus of the protein (Figure 1).

The indole amine of Trp-26 resides in the 19 amino acid hydrophobic core of the M13 coat protein (Figure 1), where backbone amides have been observed to exchange slowly (O'Neil & Sykes, 1988; Henry et al., 1987). As Figure 2

shows, the indole NH exchanges slowly enough that its exchange rate can be estimated directly by the exchange into D_2O technique; at pH* 7.1 the indole NH exchanges about 200-fold slower than the rate of exchange of tryptophan in model peptides at its pH_{min} in water (Tables I and III). It is unlikely that SDS alone could retard the exchange of the indole amine [see O'Neil and Sykes (1989) and Tables II and III], so this result suggests that the fold of the polypeptide slows down exchange of the indole NH and its neighboring backbone amides either through hydrogen-bonding interactions or by some other structural mechanism. The pH^*_{min} of the indole NH is elevated by about 1.6 units compared to the pH^*_{min} of freely exchanging tryptophan in water, and this is most likely due to an electrostatic effect of the concentrated negative charges at the micelle surface. However, because exchange is retarded, it is also possible that a "hydrophobic effect" could contribute to the elevated pH^*_{min} and retardation of exchange by depressing k_{OH} to a greater extent than k_H is depressed (Perrin & Lollo, 1984; O'Neil & Sykes, 1989).

The observations from saturation-transfer experiments suggest that the Trp-26 indole NH exists in two environments (Figure 4B). Twenty-five percent of the intensity change corresponds to a tryptophan exchanging at approximately the same rate as a water-soluble tryptophan-containing model peptide at its pH_{min} (Tables I and III); however, the pH_{min} for this transition is about 1.7 pH units higher than the pH_{min} of the indole NH in water (Tables I and III). This exchange is much too rapid to be measured by the direct exchange-out in D_2O technique (Figure 2; Table I). Seventy-five percent of the pH-dependent loss in NH intensity by saturation transfer corresponds to an indole NH exchanging about 1000-fold slower than a freely exchanging tryptophan and with a pH_{min} elevated by about 1.9 pH units. This is similar to the exchange measured in D_2O (Figure 2), but in D_2O exchange is slower by only 200-fold compared to the exchange of free tryptophan. The reason for the difference in these two measurements as well as the origin of the two transitions is not known. Clearly, the slow exchange measured by saturation transfer is not due only to pH-dependent conformational changes in the protein because the experiment in D_2O reveals a slowly exchanging indole NH at pH values near neutrality (Figure 2; Table I). However, the pH dependence of saturation transfer is not completely reversible, which suggests that pH-dependent conformational changes may explain the difference in rates measured for the slow components by the two different experiments.

One difference between the two experiments was the protein concentration; in the direct exchange-out experiments the protein was about 1.5 mM, whereas in the saturation-transfer experiments it was 2.7 mM. This difference might be important since the protein is well-known for its tendency to aggregate (Makino et al., 1975; Datema et al., 1987a,b; 1988; Cavalieri et al., 1976). Makino et al. (1975) used sedimentation equilibrium in which protein concentration ranged from 0.02 to 0.2 mM to show the protein is a dimer in SDS. In addition, many of the [^{13}C]carbonyl resonances appear as doublets in the NMR spectra of labeled protein at about 1 mM, and this also suggests dimerization (Henry et al., 1986, 1987a,b; Henry & Sykes, 1989). If the dimer is asymmetric, it might be possible for half of the tryptophans to exchange rapidly because they are exposed to solvent, while the other half of the indole amines would exchange more slowly owing to their location at the interface between two tightly associated monomers. And since self-association of the protein must be concentration dependent, it is possible that at higher concentrations the dimers associate further. The temperature dependence of the indole amine chemical shift measured by Cross and Opella (1981) (0.006 ppm/°C) suggests that the NH is not hydrogen-bonded and that its slow exchange is due to solvent inaccessibility as might be expected at the interface of associated hydrophobic proteins. It is interesting to note that the Gln-15 pH titration (Figure 4A) shows no evidence of multiple transitions despite the fact that the results from Trp-26 and Gln-15 were obtained from the same experiment.

Exchange from Peptides in Detergents. There are at least two ways in which detergents might affect hydrogen exchange in detergent-solubilized peptides. The electrostatic potential near the surface of an ionic micelle will alter the concentrations of the hydrogen-exchange catalysts. For example, near the surface of an SDS micelle the electrostatic potential will elevate [H_3O^+], enhancing k_H, and decrease [OH^-], thereby supressing k_{OH}. The effect on each ion should be equal in magnitude but opposite in direction, resulting in a net shift in the pH_{min} for exchange without either depressing or elevating the k_{min}. Another possible effect of detergents is the "hydrophobic effect": Because of the difficulty of solvating charged transition states, k_{OH} and k_H will be depressed in a hydrophobic environment [see Perrin and Lollo (1984)]. However, depending upon the details of the catalytic mechanisms, k_{OH} and k_H may be depressed to different extents, which can result in reductions in k_{min} as well as shifts in pH_{min}.

Tables II and III show that all of the primary amide and indole amine protons of the three peptides exchange in SDS with pH_{min} that are higher than the corresponding pH_{min} in water. Since none of the k_{min} are depressed (they are all slightly elevated), this suggests that the major effect of SDS is an electrostatic one and is the result of a lower pH near the surface of the micelle. The range of pH_{min} shifts (0.38–1.05) is most likely due to a variation in the affinities of the peptides for SDS as well as the positions of the exchanging protons relative to the surface of the micelle. In this regard it is somewhat surprising that the anionic *N*-acetyl-Trp-Phe interacts with the micelle at all; that its pH_{min} values are shifted suggests that the hydrophobic attraction between the aromatic rings of the peptide and the hydrocarbon of the micelle is greater than the charge repulsion between the peptide and the detergent sulfate residues. The elevation of k_{min} for all protons in SDS is very small but nevertheless measurable. One possible explanation for this observation is that in water the hydrophobic peptides may be weakly hydrogen bonded to each other and the effect of SDS may be to disrupt these interactions and increase k_{OH}, k_H, and k_{min}.

The nonionic detergent octyl glucoside generally affects hydrogen exchange in all of the peptides to only a small extent. In each case OG shifts pH_{min} to higher pH values by 0.22–0.36 pH unit. In most cases this is due mainly to a depression of k_{OH} values, whereas the k_H values are almost unchanged. The only exception to these generalities is the exchange from the carboxyl terminus of *N*-acetyl-Leu-Gln-Ile-amide (Table II) in which OG appears to enhance k_H. However, this apparent enhancement may be due to experimental error as the difference in k_H is only slightly greater than the standard deviations of the fits. Besides, no such enhancement is observed for the carboxyl-terminal amide in *N*-acetyl-Trp-NH_2 (Table III). Little is known about the mechanism for acid catalysis of indole amines (Waelder & Redfield, 1977); however, primary amides generally exchange by the so-called N-protonation mechanism in which a positively charged transition state is involved. In a hydrophobic environment both k_H and k_{OH} should be depressed if acid and base catalysis both proceed

via charged transition states. The asymmetry in the effect of OG supports the proposal of Perrin and Lollo (1984) that in a hydrophobic environment acid-catalyzed hydrogen exchange of primary amides will proceed via the imidic acid mechanism that involves a neutral transition state.

The most convincing experiment with the positively charged detergent DTAB is its influence on the exchange from negatively charged *N*-acetyl-Trp-Phe. DTAB reduces the pH_{min} of the indole amine by almost 1 pH unit and also reduces the rate of exchange at the pH_{min} by more than 20-fold (Table III; Figure 8). The electrostatic potential at the positively charged surface of the micelle will concentrate hydroxyl ions and repel hydronium ions, causing an equal enhancement of k_{OH} and reduction of k_H. If this was the only effect of DTAB, we should observe a reduction of pH_{min} without any change in k_{min}. The marked reduction in k_{min} (Table III) suggests that the hydrophobic effect is depressing k_{OH} and masking the expected electrostatic enhancement of k_{OH}. That both the electrostatic and hydrophobic effects occur together may be a direct result of the structure of the detergent molecules; each positively charged nitrogen atom is surrounded by three methyl groups, which means that even the surface of the micelle is hydrophobic. This is in contrast to the surface of an SDS micelle, which is much more hydrophilic. The hydrophobic effect might contribute to some of the suppression of k_H. DTAB has little or no effect on the exchange kinetics of the neutral peptides (*N*-acetyl-Trp-amide and *N*-acetyl-Leu-Gln-Ile-NH_2), which probably reflects their weak interaction with this detergent.

Acknowledgments

We are grateful to Dr. Gillian Henry for many helpful discussions. We thank Gerry McQuaid for upkeep of the VXR-500 spectrometer, Dr. Robert Hodges and the Alberta Peptide Institute for providing the synthetic peptides used in this study, Dr. Joel Weiner for providing facilities for the growing of *E. coli*, and Sue Smith for typing the manuscript.

References

Allinger, N. L., Cava, M. P., de Jongh, D. C., Johnson, C. R., Lebel, N. A., & Stevens, C. L. (1976) *Organic Chemistry*, pp 260–261, Worth Publishers, New York.

Asbeck, V. F., Beyreuther, K., Kohler, H., von Wettstein, G., & Braunitzer, G. (1969) *Hoppe-Seyler's Z. Physiol. Chem. 350*, 1047–1056.

Bundi, A., & Wüthrich, K. (1979) *Biopolymers 18*, 285–297.

Cavalieri, S. J., Goldthwaite, D. A., & Neet, K. E. (1976) *J. Mol. Biol. 102*, 713–722.

Covington, A. K., Robinson, R. A., & Bates, R. G. (1966) *J. Phys. Chem. 70*, 3820–3824.

Cross, T. A., & Opella, S. J. (1980) *Biochem. Biophys. Res. Commun. 92*, 478–484.

Cross, T. A., & Opella, S. J. (1981) *Biochemistry 20*, 290–297.

Datema, K. P., Visser, A. J. W. G., van Hoek, A., Wolfs, C. J. A. M., Spruijt, R. B., & Hemminga, M. A. (1987a) *Biochemistry 26*, 6145–6152.

Datema, K. P., Wolfs, C. J. A. M., Marsh, D., Watts, A., & Hemminga, M. A. (1987b) *Biochemistry 26*, 7571–7574.

Datema, K. P., Van Boxtel, B. J. H., & Hemminga, M. A. (1988) *J. Magn. Reson. 77*, 372–376.

Eigen, M. (1964) *Agnew. Chem. 3*, 1–19.

Englander, J. J., Calhoun, D. B., & Englander, S. W. (1979) *Anal. Biochem. 92*, 517–524.

Englander, J. J., Downer, N. W., & Englander, S. W. (1982) *J. Biol. Chem. 257*, 7982–7986.

Englander, S. W., & Kallenbach, N. R. (1984) *Q. Rev. Biophys. 16*, 521–655.

Englander, S. W., Downer, N. W., & Teitelbaum, H. (1972) *Annu. Rev. Biochem. 41*, 903–924.

Forsen, S., & Hoffman, R. A. (1963) *J. Chem. Phys. 39*, 2892–2901.

Forsen, S., & Hoffman, R. A. (1964) *J. Chem. Phys. 40*, 1189–1196.

Gadian, D. G. (1982) *NMR and Its Applications to Living Systems*, pp 131–132, Clarendon, Oxford, U.K.

Glasoe, P., & Long, F. (1960) *J. Phys. Chem. 64*, 188–190.

Glickson, J. D., Philips, W. D., & Rupley, J. A. (1971) *J. Am. Chem. Soc. 93*, 4031–4038.

Gregory, R. B., & Rosenberg, A. (1986) *Methods Enzymol. 131*, 448–508.

Henry, G. D., & Sykes, B. D. (1989) *Biochem. Cell Biol.* (in press).

Henry, G. D., Weiner, J. H., & Sykes, B. D. (1986) *Biochemistry 25*, 590–598.

Henry, G. D., Weiner, J. H., & Sykes, B. D. (1987a) *Biochemistry 26*, 3619–3626.

Henry, G. D., Weiner, J. H., & Sykes, B. D. (1987b) *Biochemistry 26*, 3626–3634.

Hvidt, A., & Linderstrøm-Lang, K. (1954) *Biochim. Biophys. Acta 14*, 574–575.

Karplus, M., & McCammon, J. A. (1981) *CRC Crit. Rev. Biochem. 9*, 293–349.

Kawata, Y., Goto, Y., Hamaguchi, K., Hayashi, F., Kobayashi, Y., & Kyogoku, Y. (1988) *Biochemistry 27*, 347–350.

Keniry, M. A., Gutowsky, H. S., & Oldfield, E. (1984) *Nature 307*, 383–386.

Krishna, N. R., Huang, D.-H., Glickson, J. D., Rowan, R., & Walter, R. (1979) *Biophys. J. 26*, 345–366.

Krishna, N. R., Sarathy, K. P., Huang, D.-H., Stephens, R. L., Glickson, J. D., Smith, C. W., & Walter, R. (1982) *J. Am. Chem. Soc. 104*, 5051–5053.

Leo, G. C., Colnago, L. A., Valentine, K. G., & Opella, S. J. (1987) *Biochemistry 26*, 854–862.

Lewis, B. A., Harbinson, G. S., Herzfield, J., & Griffin, R. G. (1985) *Biochemistry 24*, 4671–4679.

Linderstrøm-Lang, K. U., & Schellman, J. A. (1959) *Enzymes, 2nd Ed. 1*, 443–510.

Makino, S., Woolford, J. L., Tanford, C., & Webster, R. E. (1975) *J. Biol. Chem. 250*, 4327–4332.

Means, G. E., & Feeney, R. E. (1971) *Chemical Modification of Proteins*, p 214, Holden-Dayx, Toronto.

Miura, T., Takeuchi, H., & Harada, I. (1988) *Biochemistry 27*, 88–94.

Nakanishi, M., Nakamura, H., Hirakawa, A. Y., Tsuboi, M., Nagamura, T., & Saijo, Y. (1978) *J. Am. Chem. Soc. 100*, 272–275.

Nakashima, Y., & Konigsberg, W. (1974) *J. Mol. Biol. 88*, 598–600.

Narutis, V. P., & Kopple, K. D. (1983) *Biochemistry 22*, 6233–6239.

O'Neil, J. D. J., & Sykes, B. D. (1988) *Biochemistry 27*, 2753–2762.

O'Neil, J. D. J., & Sykes, B. D. (1989) *Biochemistry 28*, 699–707.

Perrin, C. L., & Johnston, E. R. (1979) *J. Magn. Reson. 33*, 619–626.

Perrin, C. L., & Arrhenius, G. M. L. (1982) *J. Am. Chem. Soc. 104*, 6693–6696.

Perrin, C. L., & Lollo, C. P. (1984) *J. Am. Chem. Soc. 106*, 2754–2757.

Perrin, C. L., Johnston, E. R., & Ramirez, J. L. (1980) *J. Am. Chem. Soc. 102*, 6299-6304.
Perrin, C. L., Johnston, E. R., Lollo, C. P., & Kobrin, P. A. (1981) *J. Am. Chem. Soc. 103*, 4691-4696.
Plateau, P., & Gueron, M. (1982) *J. Am. Chem. Soc. 104*, 7310-7311.
Richarz, R., Sehr, P., Wagner, G., & Wüthrich, K. (1979) *J. Mol. Biol. 130*, 19-30.
Tüchsen, E., & Woodward, C. (1987) *Biochemistry 26*, 8073-8078.
Waelder, S. F., & Redfield, A. G. (1977) *Biopolymers 16*, 623-629.
Webster, R. E., & Cashman, T. S. (1978) in *The Single Stranded DNA Phage* (Denhardt, D. T., Dressler, D., & Ray, D., Eds.) pp 557-569, Cold Spring Harbor Laboratory, Cold Spring Harbor, NY.
Wedin, R. E., Delepierre, M., Dobson, C. M., & Poulson, F. M. (1982) *Biochemistry 21*, 1098-1103.
Woodward, C. K., & Hilton, B. D. (1979) *Annu. Rev. Biophys. Bioeng. 8*, 99-127.

Detergent Modification of Myosin Function and Structure in Solution†

Stefan Highsmith
Department of Biochemistry, School of Dentistry, University of the Pacific, San Francisco, California 94115
Received March 20, 1989; Revised Manuscript Received April 26, 1989

ABSTRACT: Rabbit skeletal muscle myosin and myosin subfragment 1 (S1) MgATPase activities were increased 2-3-fold by the addition of a variety of molecules that contained single straight saturated 12-16-carbon chains. The nonionic detergent dodecyl nonaoxyethylene ether ($C_{12}E_9$) increased the activity of S1 to 50% of maximum at a free $C_{12}E_9$ concentration of 27 ± 9 μM. The activation was reversible and was not due to chemical modification of S1 amino acid side chains. The V_{max} for actin-activated S1 MgATPase activity was increased 3-fold by $C_{12}E_9$. The apparent association constant for S1 binding to pure F-actin was reduced 3-fold by $C_{12}E_9$. The [$C_{12}E_9$] dependencies of the increase in S1 and acto-S1 MgATPase activities and of the decrease in acto-S1 binding were equal, within experimental uncertainty, suggesting that a single detergent-induced S1 conformational change is sufficient to explain the results. The stoichiometry of $C_{12}E_9$ bound to S1 in the S1-$C_{12}E_9$ complex was estimated, by the S1 concentration dependence of the $C_{12}E_9$ activation midpoint and by the light-scattering increase when S1 and detergent were mixed, to be 7 and 57 $C_{12}E_9$ molecules per S1, respectively. The results are discussed in relation to possible structural aspects of the mechanism of action for S1 and acto-S1 MgATPase activities.

Actin binding accelerates the rate of MgATP hydrolysis by myosin in solution by 1 or 2 orders of magnitude, depending on the conditions. Presumably, actin activation is a manifestation of the mechanism of energy transduction by which actomyosin in muscle uses energy from MgATP binding and hydrolysis to produce force. By investigating the activation of myosin, by actin or by other molecules, one hopes to gain insight into the transduction mechanism. Activation by organic molecules received attention a few decades ago but has not been studied much recently. Aliphatic alcohols with from one to four carbons were shown to increase the rate of myosin or myosin subfragment 1 (S1)[1] activity (Laidler & Ethier, 1952; Ebashi & Ebashi, 1959; Kay & Brahms, 1963; Stone & Prevost, 1973), as were some small ethers (Laidler & Ethier, 1952; Brahms & Kay, 1962; Tonomura et al., 1963; Yasui & Watanabe, 1965). The increase in the rates of CaATP, MgATP, or KATP hydrolysis by myosin or myosin subfragment 1 (S1) is from 1.2- to 5-fold for these small water-miscible organic molecules.

In general, the more hydrophobic molecules are more potent activators. For the one- through four-carbon alcohols, the longer and less branched the hydrocarbon chain, the lower the concentration at which it is effective at increasing the rate of hydrolysis (Ebashi & Ebashi, 1959). However, in all cases, relatively high concentrations (0.1-10 M) of the cosolvent were required for maximum activation, which was typically followed by irreversible inhibition at higher concentrations. The data were interpreted in terms of modifier-induced conformational changes of myosin (Rainford et al., 1964), although evidence for myosin secondary structural changes was not obtained. For example, dioxane at about 1 M increases the CaATPase activity of myosin 1.4-fold, but no structural changes were detected by optical rotary dispersion (Tonomura et al., 1963).

Reported here are the results from recent measurements on the effects of somewhat larger organic molecules on the MgATPase activity of myosin and actomyosin. In particular, the nonionic detergents of the alkyl polyoxyethylene ether type (C_XE_Y), and related structures, were found to increase myosin, S1, and acto-S1 MgATPase activities 2-3-fold, and to reduce the affinity of S1 for F-actin. This effect on activity is different from those reported recently for other amphipathic molecules which are inhibitory (Toste & Cooke, 1979; Davies, 1980) or benign (Reisler & Liu, 1981; Borejdo, 1983) with regard to activity. It appears that most of the activation observed in the present case is due to the long unbranched saturated hydrocarbon portion of the detergent. As the alcohol results in the literature suggest, the activation of S1 by these longer chain hydrocarbon structures is observed at much lower concentrations than were observed for the shorter chain molecules. S1 is activated by $C_{12}E_9$ and related structures in the 20-70

†Supported by NIH Grant AR 37499.

[1] Abbreviations: S1, myosin subfragment 1; ATP, adenosine 5′-triphosphate; C_XE_Y, *n*-alkyl polyoxyethylene ether with *X* carbons in the alkyl chain and *Y* ethylene glycol units in the polyoxyethylene chain.

0006-2960/89/0428-6745$01.50/0